www.idosr.org Ese and Obiekezie
©IDOSR PUBLICATIONS
International Digital Organization for Scientific Research
IDOSR JOURNAL OF COMPUTER AND APPLIED SCIENCES 6(1):54-65, 2021. ISSN: 2579-0803

Depth of Induction of the Equatorial Electroject in the African Region using Solar Quiet (Sq) Field Variation

Ese Lawrence Esiekpe and T. N Obiekezie
Email: tejiriandfejiro@gmail.com
Department of Physics and Industrial Physics,Nnamdi Azikiwe University Awka.

ABSTRACT

The depth of induction of the Equatorial electrojet current to electrical conductivity of the subsurface of the solid earth in the region of Africa was determined using naturally geomagnetic variation on quiet days generated by fluctuating electric current in the ionosphere. The study used magnetic data collected from records of magnetic observatories located in the region of Africa: Ilorin(4.68⁰N, 8.50⁰E), Addis Ababa (9.04⁰N,38.77⁰E), Algeria (36.85⁰N, 2.93⁰E) and Khartoum (15.33⁰N, 32.32⁰N) acquired by SuperMag magnetic data centre in the year 2011. The EEJ strength was estimated by subtracting variation in horizontal component geomagnetic field of stations located off the EEJ strip from the daily variation in horizontalcomponent of stations located within the EEJ strip.The internal and external field contributions to the variations in Sq(H) was separated using spherical harmonics analysis (SHA).A transfer function was employed in estimating the conductivity-depth profile for the external and internal paired coefficients of the Spherical Harmonics Analysis (SHA).The electrojet current was observed to penetrate the lower mantle to depth of about 1092km in the African region. The conductivity–depth structure was observed to increase downward with a high conductivity observed within depth of 116km and 326km, which is liken to seismic low velocity region. Findings also reveal conductivities to be below1.5S/m below 600km increasing up to about 2S/m at the lower mantle.

Keywords: Induction, Equatorial, Electroject, African Region, Solar Quiet, Field Variation

INTRODUCTION

The variation of the magnetic field of the earth has large spectrum coverage and period that ranges from few seconds to millions of years [1,2]. The variations that take place over a period of years are called geomagnetic secular changes and are known to have their origin in the earth's outer core.The changes in the earth's magnetic field that are short termed are known as transient variation and have their origin from currents flowing in the ionosphere and the magnetosphere according to [3,4]. Currents flowing in the magnetosphere and ionosphere causes geomagnetic storms and suvstoms. The changes in the earths' magnetic field observed on magnetic quiet days are the smoothest and most regular and are known as solar quiet (Sq) daily variations [5]. Solar quiet daily variation is one of the transients geomagnetic changes attributed to solar events and oher number of related phenomena of the upper atmosphere [6]. [7] showed that an abnormally largedaily variation usually two or three fold enhancement in Sq (H)occurs within a narrow range of dip latitude centered over the magnetic equator within a narrow belt of latitudes(±3°) over the dip equator), and was named Equatorial Electrojet. [8] pointed out that an east-ward current flowing in the E-region of the ionosphere causes the electrojet. The electrojet strength in a givenlocation is computed by subtractingthe daily variation of X or Hcomponent of the earth's magnetic field at off equatorial stations from the daily variation of Hor X component of the geomagnetic fieldat the equatorial (EEJ) station, in thesame longitudinal zone. The enhancement in the Sq (H) daily variation in the earth's magnetic field observed at equatorial stations are of great significance. This is due to its close association with solar weather condition. According to Baker and Martyn 1953 , a huge east-ward conductivity due to the electric and magnetic field intersecting at right angle at the dip equator, is the cause of the equatorial electrojet current.with the normal Sq electric field [9]. The flowing current in the ionosphere induce magnetic perturbation on the ground. The nature of the head currents together with the spread of electrically conducting materials in the solid earth, determines the extent of penetration, magnitude as well as the direction of the induced current. Magnetometers in geomagnetic observatories on the earth surface record a hybrid of the head current (external) and the induced (internal) field parts of the currents. The couduxtivity of the solid earth can be obtained by separating the external (head) current and the induced internal current into their separate parts with the help of spherical harmonic analysis technique and other techniquesaccording to [10]. The conductivity -depth structure of the solid earth has been obtained in time past using different geophysical methods amongst them are; seismic, gravity, resistivity methods, aeromagnetic techniques. Older workers including [11,12,13] noted that these methods are limited to depth of 200 Km from the earth crust. The large physical energy required and the complications involved in these techniques were also emphasized.The integration of the upper atmosphere with the solid Earth using slowly naturallytime varying geomagnetic field arising fromunsteady currents in the upper atmosphere is known to be a useful tool in profiling the conductivity –depth structure of the deep earth to greater depth. The current derived from changes in the earth's magnetic field obtained from a long period of geomagnetic variation can be used to investigate the conductivity of the earth to a depth range of 200- 1500 km according to [11]. Previous works on profiling conductivity depth structure in Africa including the work of [14,15] have used Sq current in profiling conductivity depth structure in the African region. They found intriguing resultsthat have helped in understanding the solid Earth interior. For example [16], worked in the African region and found conductivity that increases downwards.They reported a high conductivity at depth of 100km and 205 km corresponding to seismic low velocity region. Also, [16] worked in Malaysia.They determined the mantle electrical conductivity depth structure of Malaysia using Sq currents.They reported a conductivity that increases downwards. The aim of this work was to extract the narrow band electroject current from the Worldwide Sq in the African region to profile the depth of induction of the equatorial electrojet currentto subsurface conductivity in the African region using natural geomagnetic variation.

Data Source

In this work, geomagnetic data recorded by magnetometers in observatories installed in Africa (Ilorin (4.68° N, 8.50° E),Algeria (36.85°N, 2.93°E), Addis Ababa (9.04°N, 38.77°E) andKhartoum (15.33°N, 32.32° E) acquired by Supermagnetic data centerfor the year2011 were used.The stations includes two stations within the influence of the EEJ (Ilorin and Addis Ababa) and two stations outside the EEJ influence which are Algeria and Khartoum.

Stations under study

Four stations in the African region were used for the purpose of the study. Two of the stations are off the equatorial electrojet influence (latitude ±3° over the equator) which are Medea ($A0_2$) in Algeria and Khartoum in Sudan (KRT). The other two stations are within the influence of the equatorial electrojet current: Ilorin in Nigeria (ILR) and Addis Ababa (AAE) as shown in Fig 1 below.The thick line in Fig 1 represents the equator. The geographic and geomagnetic coordinates of the stations and their code are in Table 1 below.

Table 1 Stations and their coordinates.

s/n	Station	Code	Country	GeogrLat	Geographic Longitude	Geomagnetic Latitude	Geomagnet Long
1	Ilorin	ILR	Nigeria	8.50	4.68	-1.25	76.73
2	Algeria	AO2	Algeria	36.85	2.93	27.98	77.67
3	AddisAbaba	AAE	Ethiopia	9.04	38.77	0.77	110.94
4	Khartoum	KRT	Sudan	15.33	32.32	5.69	103

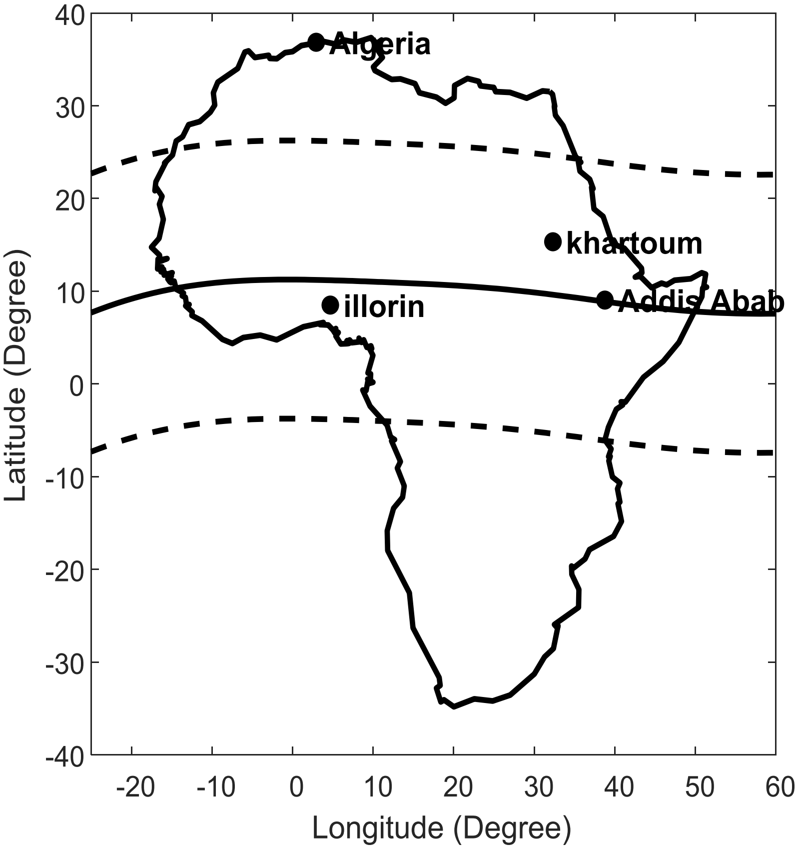

Fig 1: Geographical map of the stations

Method of Data Analysis

First, magnetically quiet days was selected using the 2011 planetary geomagnetic disturbance K_p index. The maximum value for each day of 2011 was used to select five magnetically quiet days in each month of the year, making a total of sixty quietest days as shown in Table 1.The five quietest days used were those which have the greatest value of the planetary geomagnetic disturbance index is less than or equal to 2 .The data used were minute by minute data which were converted to hourly value (24hrs) for each of the five selected days.The hourly value for each of the five selected quiet dayswere summed up and their average calculated. The result is the 24-hourly average for each month of the year for the horizontal component of the geomagnetic field. The mean values of horizontal component of the geomagnetic field of the four hours flanking midnight were used as the baseline in this work. The hourly departure from the midnight baseline was computed for the horizontal component geomagnetic field and non – cyclic variation to obtain the solar quiet daily variation in the horizontal component geomagnetic field Sq (H) shown in Table 3a-

b. The EEJ strength was obtained by subtracting solar quiet variation in horizontal component of the geomagnetic field at a station off the EEJ influence from a station within the EEJ strip. The two stations must lie in the same or close longitude in accordance with [17]. Spectral (Fourier) analysis was carried out obtaining spectral analysis (4 harmonics) of each Fourier (sine and cosine) coefficients for the year under study (2011). Thereafter, spherical harmonic analysis (SHA) was carried out, obtaining the Legendre polynomial external and internal coefficients. [18], devised a means of computing the depth (d) in km to equivalent layer of conductivity(σ) in S/m, that can produce the observed field measurement at the Earth surface for each SHA coefficients of degree n and order m. Campbell and Anderssen (1983) generalized this form and [19] modified this as:

$$C_n^m = z - ip \qquad 1$$

“This forms a complex number in which the real (z) and the imaginary (-p) parts are given by” [6]:

$$Z = \frac{R}{n(n+1)}\left\{\frac{A_n^m\left[na_n^{me} - (n+1)a_n^{mi}\right] + B_n^m\left[nb_n^{me} - (n+1)b_n^{mi}\right]}{(A_n^m)^2 + (B_n^m)^2}\right\} \qquad 2$$

$$p = \frac{R}{n(n+1)}\left\{\frac{A_n^m\left[nb_n^{me} - (n+1)b_n^{mi}\right] - B_n^m\left[na_n^{me} - (n+1)a_n^{mi}\right]}{(A_n^m)^2 + (B_n^m)^2}\right\} \qquad 3$$

where R is the Earth’s radius in km, z and p are given in km and the coefficient sums are also given by the equation $a_n^{me} + a_n^{mi} = A_n^m$ and $b_n^{me} + b_n^{mi} = B_n^m$.

The depth to substitute layer in km for each pair of coefficients is given by :

d_n^m = z - p . $\sigma_n^m = \frac{5.4\ x10^4}{m(\pi p)^2}$ S/m

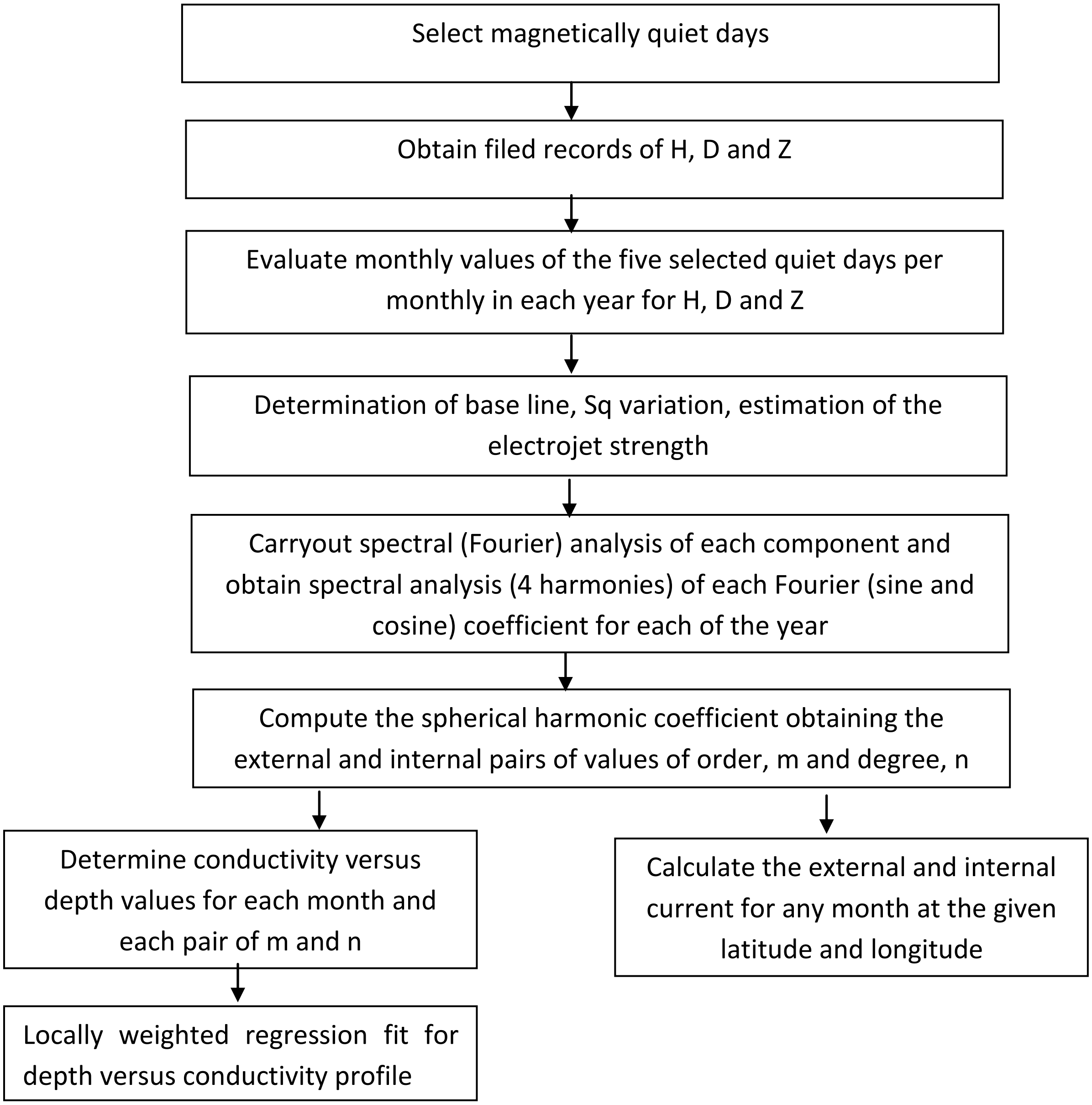

Fig 2: Data processing flow chat

RESULTS AND DISCUSSION

Table 1: Geomagnetic quiet days and their K_p values for 2011

Jan K_p	23 0_+	30 0_+	5 1_+	27 1+	21 2-
Feb Kp	3 0+	9 1	27 1	13 1	28 1
Mar K_p	15 0+	26 0+	16 1-	18 1	27 1
Apri K_p	26 1-	27 1-	10 1	16 1	26 1+
May Kp	20 1-	8 1	15 1	12 1+	9 1+
Jun K_p	29 1-	3 1	19 1+	27 2-	28 2-
Jul K_p	27 1+	28 1+	16 1+	24 1+	17 2-
Aug K_p	31 1-	3 1	18 1	19 1	21 1+
Sept K_p	23 1-	16 1	19 1	1 1+	8 2-
Oct K_p	28 0+	29 0+	22 1-	14 1-	23 1
Nov K_p	14 0+	19 0+	9 1-	20 1-	13 1
Dec K_p	27 0	16 0+	26 0+	17 1-	6 1-

JANUARY				FEBUARY				MARCH				APRIL				MAY				JUNE		
A02	KRT	ILR	AAE	A02	KRT	ILR	AAE	A02	KRT	ILR	AAE	AO2	KRT	ILR	AAE	A02	KRT	ILR	AAE	A02	ILR	AAE
-1.0745	-1.6565	-1.471	-1.3585	-3.045	-2.364	-4.052	-3.2515	-0.9765	0.0255	-1.556	-3.427	-0.85813	-0.0695	0.755625	-0.3195	-4.91138	-3.113	-4.773	-2.1545	-2.675	-4.995	-2.04863
-0.76528	-0.84224	-0.92961	-1.28589	-3.23074	-2.44878	-4.00426	-2.03333	-1.70998	0.150717	-1.82078	-0.75491	-1.89693	-0.18915	0.383973	0.171283	-1.5714	-5.22326	-2.17726	-4.58807	-3.40674	-3.80761	-1.46289
-1.59807	-1.34198	-1.38822	-0.41128	-3.61048	-1.89357	-4.05852	-2.27315	-1.51546	0.711935	-1.71757	-0.00883	-1.10073	-0.5628	1.484321	-0.05594	-3.04742	-5.62952	-3.01952	-6.63963	0.001522	-6.01022	-1.27515
-0.25485	-0.64172	-0.27083	-1.04267	-3.71622	-1.62435	-3.89078	-2.33498	-1.15094	0.175152	-1.91835	-0.32474	-0.62954	-0.30046	2.320668	-1.28515	-4.53594	-2.75778	-3.26578	-7.8412	-0.44022	-7.20283	-0.82541
1.34437	-1.14146	0.590565	-1.00607	-2.64796	-1.39513	-3.12704	-2.8128	0.229587	0.27837	-1.02913	-2.33865	-0.64834	0.985891	2.609016	-2.97637	-2.66696	-2.79204	-1.18804	-6.36076	2.328043	-4.12544	-2.19967
3.103587	0.668804	0.767957	-1.81546	-0.0557	-0.54991	-1.8753	-3.70663	1.422109	0.587587	-0.91391	-4.55057	0.775353	2.642239	3.323364	-4.09159	-0.13798	-1.6023	0.625696	-8.29233	-0.6037	3.191957	-4.04793
5.216804	3.669065	3.157348	-0.29285	4.188565	3.579304	1.440435	-3.06246	3.94663	3.834804	0.103304	-9.10448	2.024049	7.190587	9.527712	-5.4748	-2.39901	5.333435	2.381435	-8.39189	-8.68544	13.79935	2.00781
7.870022	8.381326	12.26874	3.883761	8.300826	13.47652	12.03417	5.027717	6.491152	11.88202	11.67652	-9.93839	2.425245	18.04694	27.27206	4.575978	-5.67253	15.93517	11.98317	-4.27946	-10.2472	32.15674	10.17955
6.857239	15.66759	26.34613	16.30837	10.61109	25.80374	28.73591	24.75589	10.26167	27.51924	32.88774	14.0697	4.01394	36.07928	50.60841	40.65476	-5.71355	30.52491	30.21491	19.39898	-6.19891	47.43413	25.14529
-1.71554	25.49785	42.76152	38.78498	13.42135	38.96896	43.32365	52.76807	17.0022	44.31446	53.25896	53.55578	7.050136	53.00763	73.75676	87.39554	-2.43707	45.36065	48.04465	52.93141	1.199348	55.68152	43.19703
-11.6923	33.96611	53.69091	61.44159	13.53961	46.27217	50.63139	73.30024	22.21672	57.26967	66.76217	83.77587	10.94633	63.24398	87.1371	112.3383	5.566908	53.06439	60.84839	81.47985	9.757609	57.16891	54.72477
-11.6951	36.94837	52.6443	69.8302	11.34187	47.75139	47.95913	80.15241	21.02324	62.69889	72.15739	97.14796	15.61253	65.15033	86.79545	115.2011	13.11089	53.90413	67.76013	92.17628	16.32587	48.9063	58.02051
-3.90589	33.57063	41.6077	69.1268	8.20013	43.15061	42.06087	70.82659	17.53576	60.35411	66.98861	93.09604	20.48372	60.74467	78.0558	105.3339	14.09236	49.08987	63.60587	86.46272	12.99413	30.6137	55.55225
1.155326	24.95689	25.47709	56.26541	4.664391	33.90383	34.60661	54.48476	13.63428	51.25733	53.66983	76.16613	20.32742	51.67702	61.37215	87.94067	10.23634	40.06761	50.34361	71.52315	6.772391	19.33109	45.43398
-1.09746	16.64715	11.71648	40.35402	1.522652	23.77104	25.86435	38.50094	8.812804	37.83654	37.06104	56.54022	16.99861	40.29937	42.5685	62.13546	5.025321	26.75735	31.67135	48.72559	2.470652	12.00848	27.29972
-2.83824	9.249413	4.52987	22.27463	-0.97309	16.61426	17.42809	26.31511	1.861326	22.83776	20.63026	39.7863	12.52731	27.91172	24.82734	37.23624	0.474299	14.28509	15.31109	23.99802	-2.56109	2.40587	13.03346
-2.54302	0.537674	2.561261	7.395239	-3.59683	9.703478	8.721826	16.77928	-3.58815	12.17298	9.643478	24.78639	6.286005	16.72407	12.50119	20.57702	-2.34922	3.298826	5.136826	6.322457	-9.14283	-2.23674	6.433201
-2.1458	-2.76207	1.824652	-1.85415	-4.47657	5.508696	3.945565	10.17746	-4.35763	5.278196	6.340696	12.96848	-0.4853	9.952413	7.330038	13.2198	-2.68025	-3.59344	1.264565	-2.00911	-9.18457	0.290652	5.32094
-1.42859	-3.2738	0.392043	-2.74354	-3.9363	1.907913	-0.1067	6.10163	-2.57911	2.423413	4.559913	5.012565	-3.0066	4.424761	3.973886	10.18459	-1.51627	-4.9417	1.034304	-4.59867	-5.6263	-1.76196	2.430679
-1.41537	-3.34554	-0.21857	-2.34694	-4.96204	1.40113	-3.48496	1.711804	-1.84059	1.29463	2.29113	0.174652	-2.15041	0.591109	2.672734	3.56937	-1.66229	-4.09796	1.134043	-5.52824	-6.04804	-2.19457	0.008418
-0.97615	-3.19328	-0.50117	-2.43233	-5.53378	-0.06365	-5.25722	1.151978	-0.32607	0.749848	1.614348	-1.33326	-1.10171	-1.40854	1.429082	0.116152	-2.26331	-2.52822	0.153783	-4.4758	-6.40978	-4.25717	-2.25184
0.311065	-3.18302	0.300217	-2.13772	-4.99152	-2.09444	-5.62148	-0.66585	-0.72554	0.193065	0.099565	-1.97117	-1.28302	-0.6102	0.630429	-1.56307	-1.93933	-1.90448	-0.98048	-2.62137	-4.16152	-4.28978	-1.5591
-1.07772	-2.73276	-1.12439	-1.67311	-3.36326	-2.79522	-4.46374	-2.77167	-0.54502	0.406283	-0.34722	-2.78309	-1.16182	-0.39185	0.236777	-0.60028	-3.25785	-2.27074	-2.54874	-1.75494	-3.28326	-5.64239	-0.52386
-1.0745	-1.6565	-1.471	-1.3585	-3.045	-2.364	-4.052	-3.2515	-0.9765	0.0255	-1.556	-3.427	-0.85813	-0.0695	0.755625	-0.3195	-4.91138	-3.113	-4.773	-2.1545	-2.675	-4.995	-2.04863
-0.89333	7.66625	11.38592	15.16275	1.02525	12.25917	11.36492	18.16208															

Table 2: Average monthly variation of H- component geomagnetic field for 2011.corrected for cyclic variation

Table 3: Average monthly variation of H- component geomagnetic field for 2011.corrected for cyclic variation

JULY		AUGUST			SEPTEMBER				OCTOBER				NOVEMBER				DECEMBER			
A02	AAE	AO2	ILR	AAE	A02	KRT	ILR	AAE	A02	KRT	ILR	AAE	A02	KRT	ILR	AAE	A02	KRT	ILR	AAE
-2.3625	-0.403	-0.24988	-2.0375	-2.1825	-2.231	-6.43875	-4.92138	-3.636	-0.32813	-3.8645	-2.3935	-4.4685	0.7235	-1.515	-1.35	-1.5955	-1.793	-3.014	-2.611	-1.5615
-3.93094	-1.34648	-0.89511	-2.09324	-1.64137	-2.886391	-9.00527	-5.11911	-4.14591	-3.76519	-4.00615	-2.93263	-4.38815	0.044978	-1.95744	-2.2467	-1.91385	-2.983783	-3.152	-3.85248	-2.7772
-4.17537	-2.04396	-0.07785	-1.82698	-0.81424	-1.085783	-8.39179	-4.42685	-4.74783	-5.05226	-3.0998	-4.00176	-3.6978	-0.489543	-2.07987	-3.32339	-2.6102	-2.932565	-2.738	-4.31596	-3.24489
-4.6398	-3.66144	1.571908	-1.41872	-2.86711	-1.113174	-6.96332	-3.72459	-5.84374	-4.60182	-3.21546	-5.53289	-2.78546	0.909935	-2.6403	-2.91409	-3.66254	-2.179348	-3.524	-4.15344	-3.35859
-3.03424	-5.72891	1.984168	-1.26246	-3.68598	-0.980565	-4.38984	-4.72283	-6.68165	-3.90389	-3.92511	-5.55402	-5.71711	1.975413	-2.71274	-2.94478	-6.40889	-0.70213	-3.286	-3.50091	-5.54228
-2.49667	-6.12039	2.693929	-0.1082	-4.33885	0.646043	-3.49136	-5.19657	-7.61157	-0.71595	-4.42276	-5.28915	-9.89276	4.618891	0.122826	-1.52948	-8.10524	1.873087	-1.222	-0.49639	-6.33998
-3.17911	-2.38587	0.56369	3.144065	-5.36972	-1.681348	-2.67288	-5.08281	-11.7255	1.966984	-2.17641	0.705717	-14.1724	7.23437	4.000391	7.725826	-3.28159	5.364304	5.38	8.97013	-1.08967
-7.01954	4.452652	-3.48655	15.28033	-8.11459	-8.340739	5.410598	8.625951	-8.80339	3.027418	7.689935	20.50059	-2.79807	6.873848	15.25996	26.45113	16.36607	8.953522	17.652	25.67465	12.24063
-11.448	17.37317	-9.25279	37.77859	4.392543	-13.53613	20.76908	35.15221	23.4367	-0.90915	22.33628	47.50546	30.25428	4.573326	29.75752	51.35444	49.26572	9.248739	31.048	42.46917	32.84094
-12.0864	37.2037	-10.2675	59.32085	33.24967	-12.915522	40.81255	60.40597	66.85278	1.278288	39.06063	69.43233	70.54863	4.580804	45.60309	72.77974	84.23937	5.567957	47.1	56.6417	55.57724
-6.09085	50.50822	-4.55627	71.33111	54.7988	-7.408913	55.08103	71.30473	95.13887	6.228723	53.32498	78.0412	101.879	4.726283	58.30265	80.08104	99.51502	-2.616826	56.476	64.70422	75.97554
3.958717	51.00674	5.888995	74.57937	66.03594	3.269696	59.82451	68.166	102.455	11.11416	58.13533	73.75607	106.7493	5.565761	59.85422	75.52235	93.64867	-2.635609	55.844	62.09274	81.26985

10.67628	43.36526	15.39026	69.38563	67.32307	11.806304	58.11799	55.89476	93.11904	13.12209	48.70167	59.24894	90.85367	4.253239	49.76378	60.50765	77.83233	-0.986391	47.456	48.63926	73.70415
11.71785	36.39378	22.18352	57.86989	55.1402	17.042913	51.21147	39.76102	72.17513	10.53003	35.24602	43.5618	69.05402	-1.455283	39.20135	45.47096	60.65398	-3.789174	33.632	31.62778	61.32046
8.571413	28.0803	21.37478	38.17415	33.46733	15.039522	38.40995	23.44728	52.84322	3.600462	22.32037	29.19467	51.37437	-5.405804	26.75491	32.03426	50.13363	-5.655957	23.198	19.6363	44.55476
1.688978	21.50083	15.70404	16.82441	15.59046	11.18613	24.07342	11.55104	36.1373	-0.4641	12.88872	19.16754	34.38672	-5.522326	17.51848	23.17957	37.98528	-6.340739	12.17	12.65483	30.08507
-5.03746	13.29135	8.297299	5.884674	6.489587	4.928739	10.8619	4.699799	22.70539	-2.68617	5.535065	15.09441	21.60507	-5.610848	10.35204	17.83487	24.58494	-5.801522	4.194	8.761348	16.65737
-7.70789	6.84987	2.76256	2.400935	3.992717	1.233348	1.69538	3.97106	12.17548	-1.24573	2.481413	12.17928	11.48941	-3.21937	7.545609	11.81217	16.01459	-2.648304	1.34	6.84187	11.23767
-5.57833	0.118391	1.329821	1.307196	0.317848	0.213957	-3.85114	1.182321	4.657565	1.557201	1.531761	7.344152	3.307761	-0.115891	5.803174	5.433478	8.906239	-0.743087	1.756	4.040391	7.167978
-2.82876	-3.53709	1.019082	-0.09254	-1.96302	0.246565	-4.88266	-1.32642	-0.49435	0.775136	0.378109	4.945022	0.016109	0.389587	2.806739	2.982783	4.379891	-0.64787	0.926	2.056913	4.590283
-2.0972	-2.65257	1.236342	-0.77228	-1.40589	-0.224826	-1.27419	-3.03016	-0.07626	-1.36443	-0.72754	3.323891	-0.63154	0.545065	0.162304	1.692087	1.639543	-0.802652	-0.43	0.787435	2.629087
-2.82963	-1.72804	2.053603	-0.39602	-1.55476	-1.704217	-3.06571	-3.9289	-1.45817	-0.574	-2.4252	1.848761	-1.2552	1.314543	-1.20013	0.411391	-0.6068	-1.103435	-1.728	-0.36004	1.171391
-3.78407	-1.22752	0.348864	-1.36376	-2.12963	-2.099609	-4.40723	-4.07014	-2.74609	-0.04356	-3.79685	-0.24437	-2.85085	1.612022	-1.74857	-0.8813	-1.35115	-1.102217	-2.412	-1.57352	-0.8938
-2.3625	-0.403	-0.24988	-2.0375	-2.1825	-2.231	-6.43875	-4.92138	-3.636	-0.32813	-3.8645	-2.3935	-4.4685	0.7235	-1.515	-1.35	-1.5955	-1.793	-3.014	-2.611	-1.5615

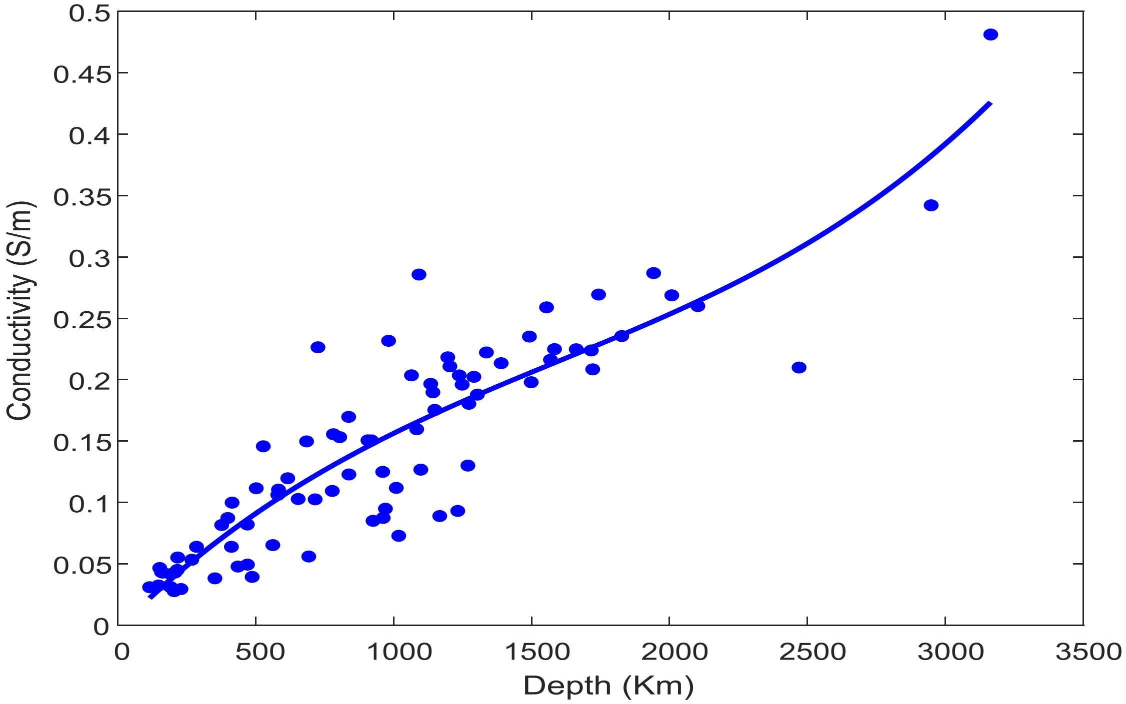

Fig 3: Depth of induction of EEJ to subsurface electrical conductivity for Ilorin/Algeria pair

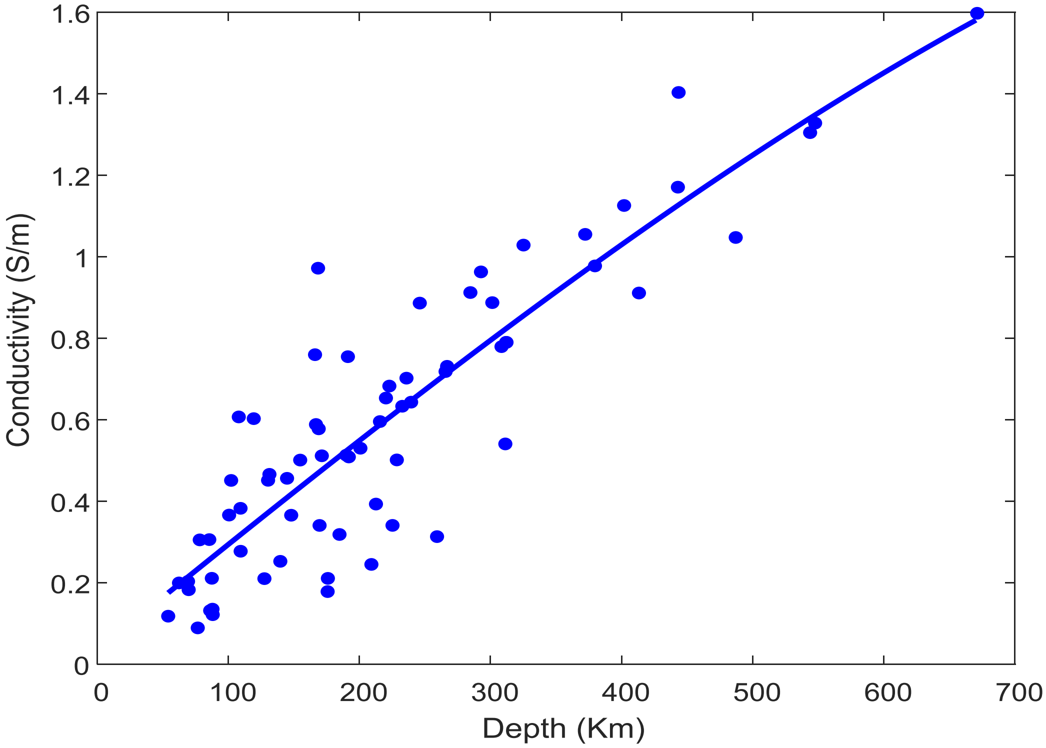

Fig 4: Depth of induction of EEJ to subsurface electrical conductivity at Addis Ababa/Khartoum pair.

Figs 3 and 4 depicts the depth of induction of the equatorial electrojet current to subsurface electrical conductivity profile of the African region based on solar quiet daily variation in the African region. The stations Ilorin (IlR) and Addis Ababa (AAE) represent equatorial latitude while Algeria ($A0_2$) and Khartoum (KRT) represent off-equatorial stations The points marked blue represent conductivity values. The conductivity –depth values are represented by the blue solid lines. Generally,the scattered points were found to be moreconcentratedwithin the crust and extend up to a depth of about 500 km and with increasing depth, the scattered points decrease. The scattered points observed differs from that reported by [20] who worked in Malaysia and reported sparse concentration of scattered points within the first few kilometers upto 450km and a more concentration of scattered points with increasing depth. "The observed scattercould be attributed to factors such as; error from the field measurements, error from the spherical harmonic analysis (SHA) fitting,variability of source current locations, and magnetic field contributionsfrom various sources other than the quiet day field" [8]. The error in profiling determination that emanates from noises in the original data and the effect of lateral inhomogeneity are verydifficult to evaluate accurately as such what could beregarded as an error is in the measurement of the regression fitting from the scattered conductivity values.Fig 2 and 3 show that the conductivity profiles increases downwards with depthfrom crustal surface deep down into the lower mantle which conforms with previouswork of [21,22,23]. The findings are expected because in the interior of the earth, temperature increases as depth increases thus, the electrical conductivity increases accordingly.The recorded profile obtained for the EEJ at Addis Ababa – Khartom pair commenced from 0.118S/m at a crustal depth of 54.28km and increased gradually to 0.607S/m at 108.1 km. It decreased to 0.178S/m at 175.88km and increased to 1.054S/m at 325.26km. It continued to increase and got to 1.403S/m at 443.54km and finally attained a maximum value of 1.597S/m at 671.27km. The profile for the EEJ at Ilorin-Algeria pair started from 0.031S/m at a depth 115.88km, rose steadily 0.04S/m at 159km.,0.063S/m at 285.9km,0.087S/m at 399.76km ,0.099S/m at 414.9km.The profile decline sharply to 0.039S/m at 487.6km and rose sharply again to 0.145S/m at 528.0km.The profile increased steadily till it attained a value of 0.226S/m at a depth of 726.04km,it declined steadily to 0.169S/m at 837.44km, 0.150S/m at 919.5km.The profile started increasing again till it attained a maximum conductivity of 0.285S/m at 1092km.The increase in conductivity at depth range between 116km to 326km in both profiles correspond to the region of low seismic velocity and high electrical conductivity [20].

CONCLUSION

Naturally slowly time varying geomagnetic daily variation on quiet days(Sqvariation)arising from fluctuating electric current in the ionosphere was used to determine the depth of induction of the equatorial electrojet current to subsurface electrical conductivity in the African region.The following deductions were made from the result:

1. The equatorialelectrojet current penetrates the solid earth upto the lower mantle to about 1092km. depth
2. The electrical conductivity increases downward attaining maximum values in the lower mantle in agreement with global models.
3. Conductivity profiles show conductivities to be about 1.5S/m below 600km, increasing upto about 2S/m at the lower mantle.
4. The rise in conductivity from the crust to about 326km coincides with seismic low velocity layers reported by previous workers.Analysis of Sq(H) variation that incorporates phenomena in the atmosphere (ionosphere) and that of the earth interior using spherical harmonic analysis has been successfully used to profile the conductivity depth structure in the African region. This no doubt will improve on the already existing knowledge of the internal structure and the physical state of the African region. Analysis of a combination of geomagnetic data of solar quiet and disturbed time variation is suggested to have a deeper understanding of the electrical behaviour of the solid earth in the African region.

REFERENCES

1. Abidin,Z.Z., Jusoh,M.H.,Abbas, M. and Yoshikawa, A.(2018). Application of solar quiet(Sq) current in determining mantle conductivity-depth structure in Malaysia, J.Atm. Sol. Terr. Phys.DOI.10.1016/j.jastp.2018.01.019
2. Arora. B. R., Campbell, W. H. and Schiffmacher, E. R. (1995) Upper Mantle Electrical Conductivity in the Himalayan Region. *J.Geomag. Geoelectr.* 47(7): 653- 665.
3. Baker, W.G. & Martyn, D.F., (1953). *The electric current in the ionosphere*, Part 1, The conductivity, Philos, Trans. Roy. So c. London, A 246, 281-294.
4. Campbell , W. H., (1997). *Introduction to Geomagnetic Fields.* Cambrige University Press, New York.
5. Campbell, W . H., (1989). The regular geomagnetic field variation during quiet solar conditions. Chap.6 in Geomagnetism. Vol 3, edtted by J.A. Jacobs pp 385-460. Academic press London
6. Campbell, W. H. & Anderssen, R. S. (1983). Conductivity of the subcontinetal upper mantle: ananalysis using quiet day records of North America*J. Geomag. Geoelectr.* 35, 367 – 382
7. Campbell, W. H., (1987). The upper mantle conductivity analysis method using observatory records of the geomagnetic field, *Pure and Appl. Geophys.*, 125, 427–457.

8. Chandrasekhar, E., 2011. Regional electromagnetic induction studies using long period geomagnetic variations. In: Petrovsky, E., Herrero-Bervera, E., , T.,Ivers, D. (Eds.), *The Earth's Magnetic Interior*, Dordrecht, Heidelberg, London, New York, vol. 1. Springer, . 31–42.
9. Chapman, S., (1951). The eq uatorial electrojet as detected from the abnormal Geophys.Bioklimatol. Ser. 4A, 368-390.
10. Egedal, J. (1947), The magnetic diurnal variation of the horizontal force near the magneticequator, *Terr. Magn. Atmos. Electr*., 52, 449 451,doi:10.1029/TE052i004p00449.
11. Keller, G.V.,(1962). Electrical resistivity of rocks in the area 12 tunnels, Nevada Test Site, nye county, Nevada. *J. Geophys. Res.* 27, 242–252.
12. Merrill, R. T., McElhinny, M. W., and McFadden, P. L.(1996).The Magnetic Field of the Earth, Paleomagnetism, the Core and the Deep Mantle, *Academic Press, San Diego,C*A.
13. Njumogo, C.N and Obiekezie, T.N. ,(2020). Upper mantle conductivity determined from the solar quiet day ionospheric currents in the equatorial and low attitudes of Africa.*Journal of Research in Environmental and Earth Sciences*.5, 45-49
14. Obiekezie, T. N. and Okeke, F. N. (2010). Upper Mantle Conductivity Determined from theSolar Quiet Day Ionospheric Currentsin the Dip Equatorial Latitudes of West Africa. *Moldavian Journal of the Physical Sciences,* 9(2): 199 – 204
15. Obiekezie, T.N.,(2012). Geomagnetic variation in the dip equatorial latitudes of West Africa. International Journal of Physical Sciences 7(36), 5372-5377
16. Obiora D. N., Okeke F. N. and Yumoto K. (2013).Determination of the crust-mantle electricalconductivity-depth structure ofNiger Delta using solar quiet day (Sq) current.*International Journal of the Physical Sciences.* 8(7):272-276.
17. Obiora, D. N; Okeke, F. N; Yumoto, K. and Agha, S. O. (2014). Mantle electrical conductivity profile of Niger delta region. J. Earth Syst. Sci. 123(4): 827–835.
18. Obiora, D., Okeke, F., 2013. Crustal and upper mantle electrical conductivity structure in North Central Nigeria. *Inter. J. Phys. Sci.* 8, 1975–1982.
19. Ohtani, E., Sakai, T., 2008.Recent advances in the study of mantle phase transitions. *Phys. Earth Planet. In.* 170, 240–247.
20. Rabiu, A. B. (2002). Seasonal Variability of Sq at Middle Latitudes.*Nig. Journ. of Phys.,* 14(I), 66-71. Research,52, 447:449.
21. Schmucker, U. (1970). An introduction to induction anomalies. *J. Geomag. Geoelectr.* 22(1-2), 9-33.
22. Ugbor, D., Okeke, F., Yumoto, K., 2016. Mapping the Earth conductivity-depth structure ofAfrican geomagnetic equatorial anomaly region using solar quiet current variations. *J. Afr. Earth Sci.* 116, 81–88
23. Ugbor,D.O and Okeke , F.N., (2017).Deep Earth Electrical conductivity-depth profiles around Africa Geomagnetic Equator using Solar Quiet currents.Geological society of India,89,344-350.